

Fluorescent Tin(IV) Complexes with Schiff Base Ligands: Synthesis, Structures, and Fluorescence Lifetime

Kentaro Takano,[1] Masayuki Takahashi,[1] Takaaki Fukushima,[1] Makoto Takezaki,[2] Toshihiro Tominaga,[2] Haruo Akashi,[3] Hideaki Takagi,[4] and Takashi Shibahara*[1]

[1]Department of Chemistry, Okayama University of Science, Ridai-cho, Kita-ku, Okayama 700-0005

[2]Department of Applied Chemistry, Okayama University of Science, Ridai-cho, Kita-ku, Okayama 700-0005

[3]Research Institute of Natural Sciences, Okayama University of Science, Ridai-cho, Kita-ku, Okayama 700-0005

[4]Department of International Conservation Studies for Cultural Properties, Kibi International University, 8 Igamachi, Takahashi, Okayama 716-8508

Received May 28, 2012; E-mail: shiba@chem.ous.ac.jp

Eleven Schiff base tin(IV) complexes of the type $[SnCl_3(L)]$ (HL: Schiff base) were synthesized and structurally characterized by X-ray crystallography and ^{1}H NMR spectroscopy, and their properties were investigated. The Schiff bases are prepared from aldehydes with a benzene or a naphthalene ring and 8-aminoquinoline or its derivatives. The complexes adopt geometries close to octahedral, with three chloride ions coordinated meridionally. Eight of the eleven tin complexes show fluorescence in DMSO, and the emission range from bluish green to orange (λ_{max}: 492–545 nm). Two solid tin complexes are fluorescent, although they are not in DMSO, and one tin complex is not fluorescent even in the solid state. The fluorescence quantum yields (Φ_f) of the complexes depend very much on the ligands ($\Phi_f = 0.21$–0.022). The fluorescence lifetimes ($\tau = 0.49$–1.76 ns) were measured and the results will be discussed. DFT calculation (B3LYP/Sn, LanL2DZ; others, 6-31G**) shows that the order of the magnitudes of HOMO–LUMO gaps is consonant with that of the emission wavelengths (λ_{max}) of the complexes. All the cyclic voltammograms of the Schiff base ligands and the complexes exhibited irreversible waves and these results suggest that the reduction products of the ligands and the complexes were unstable under the time scale in CV measurements ($0.1\ V\ s^{-1}$). Relatively good correlation was observed between reduction potentials in DMSO and the energies of LUMO.

Fluorescent compounds have attracted much attention from researchers because of their intrinsic interests and applications such as organic electroluminescence[1] and ability as tumor markers.[2] One of the Schiff bases, 2-hydroxy-1-naphthylmethylene-8-aminoquinoline (**HL1**, Chart 1), which is prepared from 2-hydroxy-1-naphthaldehyde and 8-aminoquinoline, has been used for the fluorometric measurement of Be(II),[3] Cr(III),[4] Mo(VI),[5] Pb(II),[6] and Hg(II),[7] where interfering ions, Al(III), Ga(III), In(III), Tl(III), Cu(II), have also been reported,[5,6] however, there has been no structural report of compound composed of any one of the above metal ions and **HL1** ligand has been reported to date, while the X-ray structure of **HL1** was reported recently.[8] In contrast, the X-ray structures of $[VO_2(L1)]$,[9] $[TcCl_2(L1)]$,[10] and $[FeCl_3(L1)]$[11] complexes with the ligand **HL1** were reported, but no description of fluorescence was noted. Many methods have been reported for the fluorometric determination of vanadium(V);[12] however, reports describing both the fluorescence and X-ray structure are very limited.

Recently we succeeded in determining the X-ray structure of a fluorescent Schiff base tin(IV) complex with the **HL1** ligand, and we thought it worthwhile to prepare a series of tin(IV) complexes with Schiff base ligands analogous to the ligand, since there are many kinds of derivatives of aldehydes and the combination of aldehydes and 8-aminoquinoline (and its derivatives) will give many types of Schiff base ligands, which will help investigate the tunability of the fluorescence wavelength using the Schiff base tin(IV) complexes. So far, many reports have appeared on fluorescence as described above, but it is still difficult to predict the appearance of fluorescence and their intensities of fluorescent compounds. We now report synthesis and characterization of eleven novel Schiff base tin(IV)

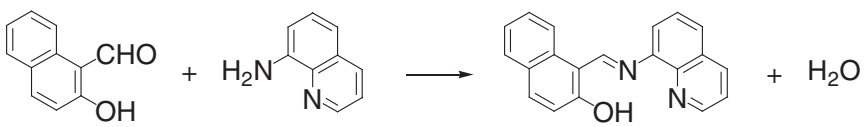

2-hydroxy-1-naphthaldehyde 8-aminoquinoline **HL1**

Chart 1. Formation of **HL1** ligand.

Published on the web November 1, 2012; doi:10.1246/bcsj.20120150

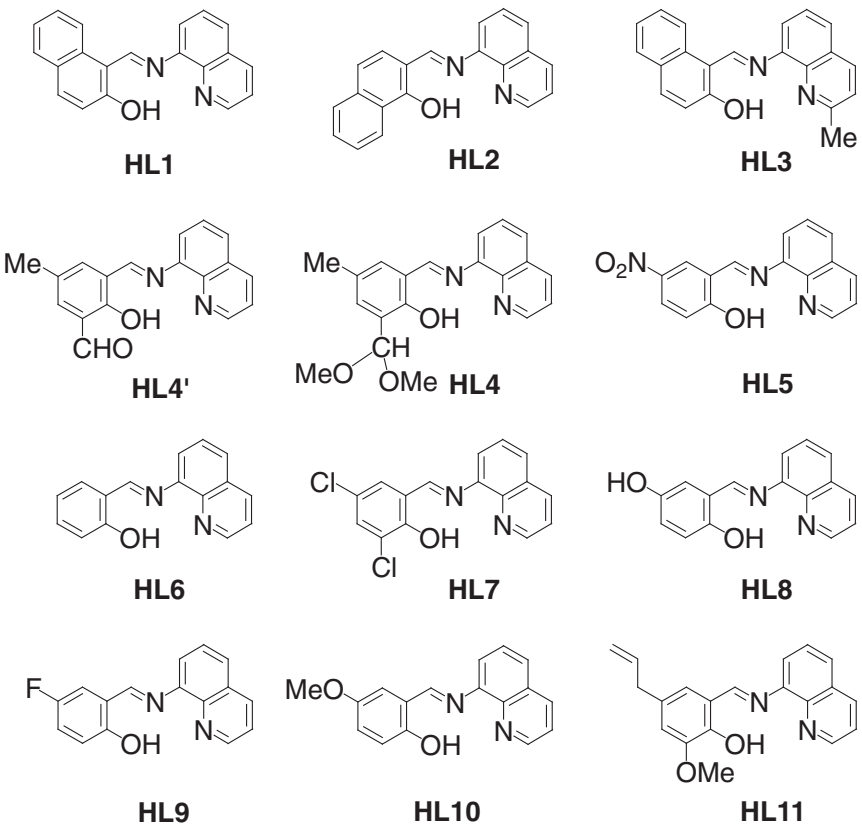

Chart 2. Schiff bases. Note: The aldehyde group of **HL4′** changes to an acetal group on coordination to tin(IV) to give **a4** (Figure S1).

complexes, $[SnCl_3(L1)]$ (**1**), $[SnCl_3(L2)]$ (**2**), $[SnCl_3(L3)]$ (**3**), $[SnCl_3(L4)]$ (**4**), $[SnCl_3(L5)]$ (**5**), $[SnCl_3(L6)]$ (**6**), $[SnCl_3(L7)]$ (**7**), $[SnCl_3(L8)]$ (**8**), $[SnCl_3(L9)]$ (**9**), $[SnCl_3(L10)]$ (**10**), and $[SnCl_3(L11)]$ (**11**), where **HL2**, **HL3**, **HL4**, **HL5**, **HL6**, **HL7**, **HL8**, **HL9**, **HL10**, and **HL11** are also Schiff bases analogous to **HL1** (Chart 2 and Table 1). Complexes **1** through **7** and complex **9** are fluorescent in DMSO, but complexes **8**, **10**, and **11** are nonfluorescent. A complex of the formula $[SnCl_3(H_2O)(L6)]$, which is close to $[SnCl_3(L6)]$ (**6**), has been reported.[13] The thermochromism of the former was reported, but fluorescence was not referred to.

As for fluorescent non-Schiff base tin(IV) complexes, organo tin(IV) complexes with 1-fluorenecarboxylic acid or 9-fluorenecarboxylic acid (Chart S1) have been reported recently together with their X-ray structures,[14] and a fluorescent tin–iridium mixed metal complex, $[Ir_2(SnCl)(CO)_2Cl_2(\mu\text{-dpma})_2][SnCl_3]$, has also been reported.[15] Incidentally, there are reports on tin(IV) complexes with the 8-aminoquinoline ligand, which is a the starting material of the Schiff base ligands, but there is no reference to the fluorescence of the complex.[16] However, there has been a report of an electroluminescent complex of diphenyltin(IV) complex with an 8-aminoquinoline ligand.[17] A preliminary report of portions of this work has appeared.[18]

Experimental

Materials and Reagents. Chemicals were used as purchased: $SnCl_4 \cdot 5H_2O$, DMSO, and DMF for fluorescence analysis, Nacalai Tesque; 8-aminoquinoline, 8-amino-2-methylquinoline, 2-hydroxy-1-naphthaldehyde, 1-hydroxy-2-naphthaldehyde, 2-hydroxy-5-methylisophthalaldehyde, 5-nitrosalicylaldehyde, salicylaldehyde, 3,5-dichlorosalicylaldehyde, 2,5-dihydroxybenzaldehyde, Tokyo Kasei; $[Al(C_9H_6NO)_3]$ (**Alq$_3$**) and DMSO-d_6(99.9%), Aldrich; $(n\text{-}C_4H_9)_4NPF_6$, Merck.

Table 1. Designations of Ligands

Schiff base ligands	
2-Hydroxy-1-naphthylmethylene-8-aminoquinoline	**HL1**
1-Hydroxy-2-naphthylmethylene-8-aminoquinoline	**HL2**
2-Hydroxy-1-naphthylmethylene-8-amino-2-methylquinoline	**HL3**
3-Formyl-2-hydroxy-5-methylbenzylidene-8-aminoquinoline	**HL4′**
2-Hydroxy-3-dimethoxymethyl-5-methylbenzylidene-8-aminoquinoline	**HL4**
5-Nitrosalicylidene-8-aminoquinoline	**HL5**
Salicylidene-8-aminoquinoline	**HL6**
3,5-Dichlorosalicylidene-8-aminoquinoline	**HL7**
5-Hydroxysalicylidene-8-aminoquinoline	**HL8**
5-Fluorosalicylidene-8-aminoquinoline	**HL9**
5-Methoxysalicylidene-8-aminoquinoline	**HL10**
5-Allyl-3-methoxysalicylidene-8-aminoquinoline	**HL11**

Measurements. Electronic spectra were measured using Hitachi U-2000 and -2800 double-beam spectrophotometers. Fluorescent spectra were measured using a Hitachi F-2000 spectrophotometer. ^{1}H NMR spectra were obtained with a Bruker ARX-400R spectrometer. Elemental analyses were determined with a Perkin-Elmer 240 NCH analyzer. Fluores-

cence decays were measured using an apparatus including a femtosecond laser system and streak camera.[19] The second harmonic of a femtosecond Ti:sapphire laser (Spectra-Physics, Tsunami 3960, wavelength of pulse: ca. 800 nm, fwhm of the pulse: ca. 80 fs) pumped by the SHG output of a Nd, YVO_4 laser (Spectra-Physics, Millennia-V) was used to excite the complexes. The detected fluorescence was dispersed by a monochromator and measured using a streak scope (Hamamatsu, C4334). The fluorescence signals were averaged using a PC. Fluorescence decay measurements were performed at 22 °C for the complexes.

Syntheses. Syntheses of Schiff Base Ligands: **HL1** was prepared according to a modified literature procedure:[5] 2-hydroxy-1-naphthaldehyde (540 mg, 3.0×10^{-3} mol) and 8-aminoquinoline (432 mg, 3.0×10^{-3} mol) were added to methanol (5 mL), which was heated at 50 °C for two hours. Allowing the the solution to stand at 50 °C gave orange plate-like crystals: yield 879 mg (98%). Anal. Found (calcd for $C_{20}H_{14}N_2O$, MW: 298.34) C, 80.36 (80.52); H, 4.81 (4.73); N, 9.40 (9.39)%.

Similar procedures to that for **HL1** were used for the syntheses of Schiff base ligands from **HL2** through **HL5**, **HL7**, **HL8**, and **HL10** using equimolar amounts of aldehydes and amines: 8-aminoquinoline was used except for **HL3**, where 8-amino-2-methylquinoline was used. Methanol was used as solvent unless otherwise noted. **HL6**, **HL9**, and **HL11** were not isolated. The following products (yields) and analytical results were obtained.

HL2·0.3MeOH (using 1-hydroxy-2-naphthaldehyde): bright-orange plate-like crystals (61%). Anal. Found (calcd for $C_{20.3}H_{15.2}N_2O_{1.3}$, MW: 307.95, MW_{HL2}: 298.34): C, 79.54 (79.43); H, 4.96 (4.66); N, 9.26 (9.13)%. The crystals seemed efflorescent.

HL3 (using 8-amino-2-methylquinoline): orange powder, which was washed with ice-cooled ethyl acetate. For recrystallization, the orange powder was recrystallized from toluene to give block crystals (66%). Anal. Found (calcd for $C_{21}H_{16}N_2O$, MW: 312.36): C, 80.53 (80.75); H, 5.10 (5.16); N, 8.95 (8.97)%.

HL4′ (using 2-hydroxy-5-methylisophthalaldehyde): red powder (52%). Anal. Found (calcd for $C_{18}H_{14}N_2O_2$, MW: 290.32): C, 74.31 (74.47); H, 4.61 (4.86); N, 9.88 (9.65)%.

HL5 (using 5-nitrosalicylaldehyde): red-brown plate-like crystals (71%). Anal. Found (calcd for $C_{16}H_{11}N_3O_3$, MW: 293.28): C, 65.58 (65.53); H, 3.76 (3.78); N, 14.29 (14.33)%. Toluene was used as the solvent.

HL7·MeOH (using 3,5-dichlorosalicylaldehyde): bright-red plate-like crystals (95%). Anal. Found (calcd for $C_{17}H_{14}N_2O_2Cl_2$, MW: 349.21, MW_{HL7}: 317.17): C, 58.03 (58.47); H, 3.73 (4.04); N, 8.21 (8.02)%.

HL8 (using 2,5-dihydroxybenzaldehyde): yellow powder (84%). Anal. Found (calcd for $C_{16}H_{12}N_2O_2$, MW: 265.29): C, 72.83 (72.99); H, 4.31 (4.21); N, 10.65 (10.64)%.

HL10 (using 2-hydroxy-5-methoxybenzaldehyde): red plate-like crystals (58%). Anal. Found (calcd for $C_{17}H_{15}N_2O_2$, MW: 279.31): C, 73.37 (73.10); H, 5.05 (5.41); N, 10.07 (10.03)%.

Syntheses of Schiff Base Tin(IV) Complexes: The following procedures were followed for the synthesis of the Schiff base tin(IV) complexes:

[$SnCl_3$(L1)] (**a1**): To a solution of **HL1** (29.8 mg, 1.0×10^{-4} mol) in acetonitrile (20 mL) at 60 °C was added a solution of $SnCl_4 \cdot 5H_2O$ (36.0 mg, 1.0×10^{-4} mol) in acetonitrile (10 mL). Keeping the mixture at 60 °C overnight gave orange crystals of **a1**: yield 20.9 mg (40%). Anal. Found (calcd for $C_{20}H_{13}Cl_3N_2OSn$, MW: 522.40): C, 46.26 (45.98); H, 2.48 (2.51); N, 5.50 (5.36)%.

[$SnCl_3$(L2)] (**a2**): To a solution of **HL2**·0.3MeOH (10.12 mg, 3.3×10^{-5} mol) in acetone (2 mL) was added a solution of $SnCl_4 \cdot 5H_2O$ (10.02 mg, 2.86×10^{-5} mol) in acetone (2 mL). Keeping the mixture at room temperature overnight gave orange crystals of **a2**: yield 8.3 mg (56%). Anal. Found (calcd for $C_{20}H_{13}Cl_3N_2OSn$, MW: 522.40): C, 46.04 (45.98); H, 2.67 (2.51); N, 5.26 (5.36)%.

[$SnCl_3$(L3)] (**a3**): To a solution of **HL3** (10.12 mg, 3.24×10^{-5} mol) in a mixture of acetonitrile (1 mL) and methanol (1 mL) was added a solution of $SnCl_4 \cdot 5H_2O$ (10.02 mg, 2.86×10^{-5} mol) in acetonitrile (1 mL). Keeping the mixture at room temperature overnight gave orange plate-like crystals of **a3**: yield 7.1 mg (46%). Anal. Found (calcd for $C_{21}H_{15}Cl_3N_2O_3Sn$, MW: 536.43): C, 47.03 (47.02); H, 2.86 (2.82); N, 5.21 (5.22)%.

[$SnCl_3$(L4)] (**a4**): **HL4′** (10.15 mg, 3.5×10^{-5} mol) and $SnCl_4 \cdot 5H_2O$ (10.0 mg, 2.9×10^{-5} mol) were dissolved in methanol (3 mL). The resultant red mixture turned to an orange solution after a few minutes of heating at 60 °C, which gave yellow powder of **a4**: yield 8.3 mg (64%). Anal. Found (calcd for $C_{20}H_{19}Cl_3N_2O_3Sn$, MW: 560.45): C, 42.32 (42.86); H, 3.20 (3.42); N, 5.08 (5.00)%.

[$SnCl_3$(L5)] (**a5**): To a slurry of **HL5** (50.11 mg, 1.71×10^{-4} mol) in methanol (20 mL) was added a solution of $SnCl_4 \cdot 5H_2O$ (10.02 mg, 2.86×10^{-5} mol) in methanol (5 mL). Keeping the mixture at room temperature overnight gave orange plate-like crystals of **a5**: yield 54.8 mg (73%). Anal. Found (calcd for $C_{16}H_{10}Cl_3N_3O_3Sn$, MW: 517.34): C, 37.02 (37.15); H, 1.78 (1.95); N, 7.98 (8.12)%.

[$SnCl_3$(L6)] (**a6**): 8-Aminoquinoline (20 mg, 1.4×10^{-4} mol), salicylaldehyde (20 μL, 1.6×10^{-4} mol), and $SnCl_4 \cdot 5H_2O$ (50 mg, 1.4×10^{-4} mol) were dissolved in acetonitrile (5 mL). Leaving the solution at room temperature overnight gave yellow plate-like crystals of **a6**: yield 19.2 mg (28%). Anal. Found (calcd for $C_{16}H_{11}Cl_3N_2OSn$, MW: 472.34): C, 40.74 (40.68); H, 2.14 (2.35); N, 5.90 (5.93)%.

[$SnCl_3$(L7)] (**a7**): To a solution of **HL7**·MeOH (10.89 mg, 3.1×10^{-5} mol) in a mixture of acetonitrile (4 mL) and methanol (8 mL) was added a solution of $SnCl_4 \cdot 5H_2O$ (10.29 mg, 2.9×10^{-5} mol) in acetonitrile (1 mL). Keeping the mixture at room temperature overnight gave yellow plate-like crystals of **a7**: yield 59.54 mg (76%). Anal. Found (calcd for $C_{16}H_9Cl_5N_2OSn$, MW: 541.23): C, 35.54 (35.51); H, 1.61 (1.68); N, 5.09 (5.18)%.

[$SnCl_3$(L8)] (**a8**): To a solution of **HL8** (7.97 mg, 3.0×10^{-5} mol) in methanol (10 mL) was added a solution of $SnCl_4 \cdot 5H_2O$ (10.0 mg, 2.9×10^{-5} mol) in methanol (1 mL). Keeping the mixture at 50 °C overnight gave red needle-like crystals of **a8**: yield 53.7 mg (73%). Anal. Found (calcd for $C_{16}H_{11}Cl_3N_2O_2Sn$, MW: 488.34): C, 39.59 (39.35); H, 2.22 (2.27); N, 5.58 (5.74)%.

[$SnCl_3$(L9)] (**a9yel** and **a9or**): 8-Aminoquinoline (13.85 mg, 9.6×10^{-5} mol), 5-fluorosalicylaldehyde (13.45, 9.6×10^{-5} mol), and $SnCl_4 \cdot 5H_2O$ (50 mg, 1.4×10^{-5} mol) were dissolved in a mixture of acetonitrile (12 mL) and water (1.25 mL). Leaving the solution at room temperature overnight gave a mixture of yellow (**a9yel**) and orange (**a9or**) crystals: yield 33.8 mg (73%). The two kinds of crystals were separated manually: the amount of **a9yel** is somewhat larger than that of **a9or**. The following analytical values were obtained: **a9yel**: Anal. Found (calcd for $C_{16}H_{10}Cl_3FN_2OSn$, MW: 490.33): C, 39.05 (39.19); H, 1.93 (2.06); N, 5.64 (5.71)%; **a9or**: Anal. Found (calcd for $C_{16}H_{10}Cl_3FN_2OSn$, MW: 490.33): C, 39.05 (39.19); H, 2.02 (2.06); N, 5.66 (5.71)%.

[$SnCl_3$(L10)] (**a10**): To a solution of **HL10** (8.01 mg, 2.9×10^{-5} mol) in methanol (10 mL) was added a solution of $SnCl_4 \cdot 5H_2O$ (9.6 mg, 2.7×10^{-5} mol) in methanol (1 mL). Keeping the mixture at 50 °C overnight gave orange needle-like crystals of **a10**: yield 5.84 mg (40%). Anal. Found (calcd for $C_{17}H_{13}Cl_3N_2O_2Sn$, MW: 502.37): C, 40.67 (40.64); H, 2.48 (2.61); N, 5.36 (5.58)%.

[$SnCl_3$(L11)] (**a11**): 8-Aminoquinoline (13.85 mg, 9.6×10^{-5} mol), 5-allyl-3-methoxysalicylaldehyde (18.25 mg, 9.6×10^{-5} mol), and $SnCl_4 \cdot 5H_2O$ (50 mg, 1.4×10^{-5} mol) were dissolved in acetonitrile (5 mL). Leaving the solution at room temperature overnight gave red needle-like crystals of **a10**: yield 19.82 mg (40%). Anal. Found (calcd for $C_{20}H_{12}Cl_3N_2O_2Sn$, MW: 542.43): C, 43.93 (44.28); H, 3.04 (3.15); N, 5.22 (5.16)%.

X-ray Structural Determinations of a1, a3, a5, a6, a7, a8, a9yel, a9or, a10, and a11. Data were collected on a Rigaku/MSC Mercury CCD diffractometer, using graphite monochromated Mo Kα radiation. Suitable crystals were attached to the tip of a glass capillary using silicone grease and transferred to the goniostat, where they were cooled at −180 °C for data collection. The structures were solved using the Patterson Method (DIRDIF99,[20] **a1**, **a3**, **a5**, **a8**, **a9yel**, **a9or**, **a10**, and **a11**) or the Direct Methods (SIR2004,[21] **a6**; SHELXS97,[22] **a7**), and all the remaining non-hydrogen atoms were located from difference Fourier maps.[23] The hydrogen atoms were also located from difference Fourier maps, and all of the isotropic thermal parameters of hydrogen atoms were constrained to $1.2U_{eq}$ to which they were attached. The program package Crystal Structure[24] was used, SHELXL being used for the refinement. Crystallographic data have been deposited with Cambridge Crystallographic Data Centre: Deposition number CCDC-656122 for **a1**, -656123 for **a3**, -661505 for **a5**, -882535 for **a6**, -882536 for **a7**, -882537 for **a8**, -882538 for **a9or**, -882539 for **a9yel**, -882540 for **a10**, and -882541 for **a11**. Copies of the data can be obtained free of charge via http://www.ccdc.cam.ac.uk/conts/retrieving.html (or from the Cambridge Crystallographic Data Centre, 12, Union Road, Cambridge, CB2 1EZ, U.K.; Fax: +44 1223 336033; e-mail: deposit@ccdc.cam.ac.uk).

Measurements of ^{1}H NMR Spectra of Schiff Base Ligands and Schiff Base Tin(IV) Complexes. Solid samples of Schiff base ligands **HL1**, **HL2**, **HL3**, **HL4′**, **HL5**, **HL7**, **HL8**, and **HL10** and tin complexes **a1**–**a11** were dissolved in DMSO-d_6, respectively, for the measurement of ^{1}H NMR at room temperature.

Measurements of Fluorescent Spectra of Schiff Base Ligands and Schiff Base Tin(IV) Complexes. **Alq_3** (1.90 mg, 4.1×10^{-6} mol) was dissolved in DMF (100 mL) and diluted 4 times with DMF to give a standard solution (1.03×10^{-5} M; 1 M = 1 mol dm^{-3}).[25] Solution samples: Schiff base ligands **HL1**–**HL5**, **HL7**–**HL8**, and **HL10** and tin complexes **a1**–**a11** were dissolved in DMSO-d_6 to make a ca. 1.0×10^{-5} M solution. In addition a 1×10^{-6} M solution of **HL4′** was also prepared for the measurement. Solid samples: Schiff base ligands or tin complexes (ca. 1 mg) were immersed with silicone oil (a few drops) on a filter paper (ADVANTEC 5C), respectively.

Electrochemical Measurement. All electrochemical measurements were performed under argon at room temperature using a Bioanalytical Systems Inc. BAS-100B Electrochemical Analyzer with a scan rate of 0.1 V s^{-1}. Each solution contained 0.5 mM sample and 0.1 M tetrabutylammonium hexafluorophosphate as a supporting electrolyte in anhydrous dimethyl sulfoxide (DMSO). A three electrode cell was employed with a platinum disk working electrode, a platinum wire auxiliary electrode, and a Ag/Ag^+ reference electrode (0.01 M $AgPF_6$ in CH_3CN). Ferrocene (Fc) was added as an internal standard and potentials are referenced versus the Fc^+/Fc couple.

DFT Calculations. The DFT calculation with the hybrid functional method (B3LYP) was carried out by using the Gaussian 03 program package.[26] We performed full structural optimization (basis sets: Sn, LanL2DZ; others, 6-31G**) starting from X-ray structures (**a1**, **a3**, **a5**, **a6**, **a7**, **a8**, **a9yel**, **a10**, and **a11**) or from molecular mechanics using Chem3D (**a2** and **a4**).

Results and Discussion

Synthesis of Schiff Base Ligands and Schiff Base Tin Complexes. Of eleven Schiff base ligands, **HL1**, **HL2**, **HL3**, **HL4′**, **HL5**, **HL7**, **HL8**, and **HL10** were isolated and used for the syntheses of tin(IV) complexes. **HL6**, **HL9**, and **HL11** were not isolated. Eleven Schiff base tin(IV) complexes were synthesized and the structures of **a1**, **a3**, **a5**, **a6**, **a7**, **a8**, **a9yel**, **a9or**, **a10**, and **a11** were determined by X-ray crystallography, which will be discussed in the next section, and those of **a2** and **a4** were determined by ^{1}H NMR spectroscopy (20 °C, 400 MHz, DMSO-d_6) (Figure S1). As to **HL4′**, the aldehyde moiety remained unchanged, though prepared in methanol: on the preparation of **a4**, the aldehyde moiety of the ligand changed into acetal.

X-ray Structures of a1, a3, a5, a6, a7, a8, a9yel, a9or, a10, and a11. ORTEP drawings of **a1**, **a3**, **a5**, **a6**, **a7**, **a8**, **a9yel**, **a9or**, **a10**, and **a11** are shown in Figure 1. The complexes adopt geometries close to octahedral: three chloride ions are coordinated meridionally, respectively. Crystallographic data and atomic distances are shown in Table 2 and Table 3, respectively. Of all the complexes Sn1–Cl1 and Sn1–Cl2 distances are clearly longer than those of Sn1–Cl3, probably because of the trans influence of chloride ion. The dihedral angle between the least-squares planes, quinoline ring and benzene (or naphthalene ring), of each complex is also listed in Table 3. There are some differences between the dimensions of **a9yel** and **a9or**.

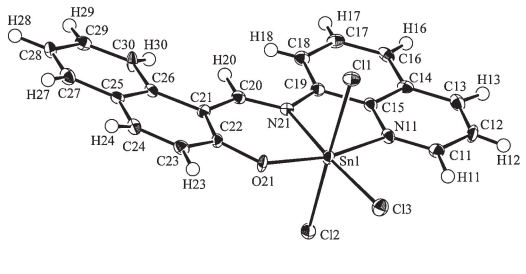

a1

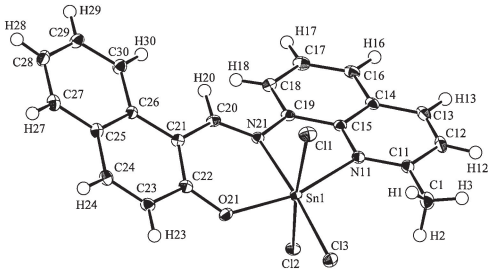

a3

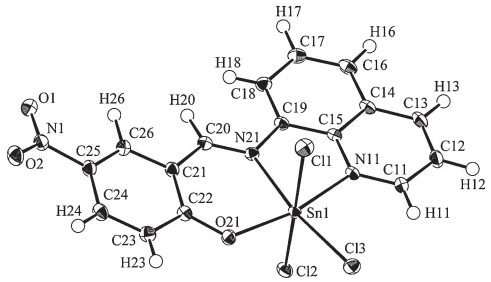

a5

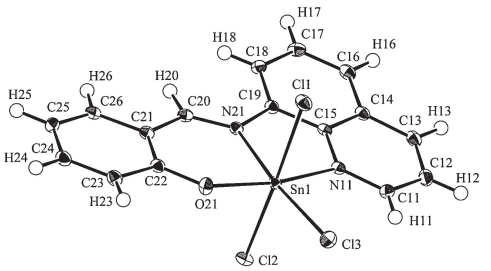

a6

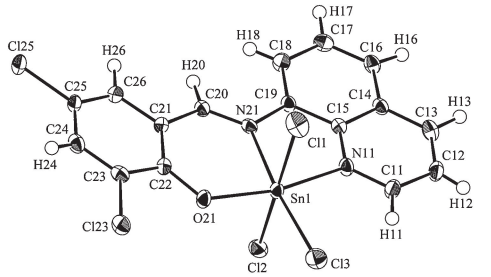

a7

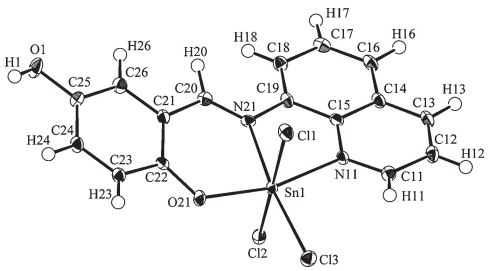

a8

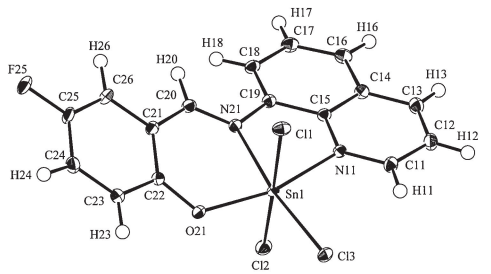

a9yel

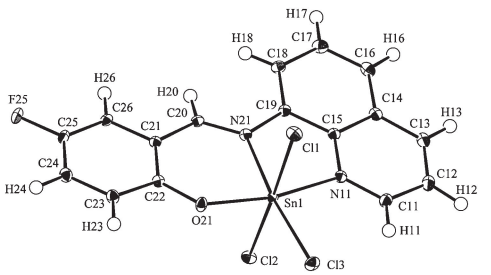

a9or

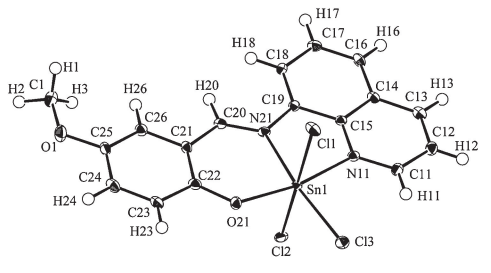

a10

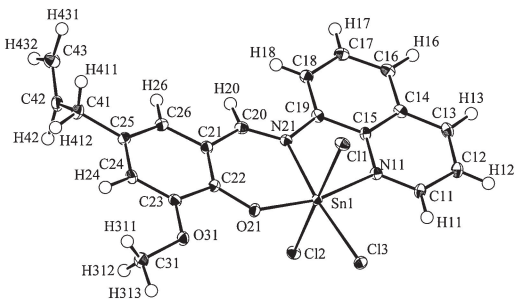

a11

Figure 1. ORTEP drawings of **a1**, **a3**, **a5**, **a6**, **a7**, **a8**, **a9yel**, **a9or**, **a10**, and **a11** with the atom-numbering schemes at the 50% probability level (see text).

Table 2. Crystal Data and Details of the Structure Determination for **a1**, **a3**, **a5**, **a6**, **a7**, **a8**, **a9yel**, **a9or**, **a10**, and **a11**

	a1	**a3**	**a5**	**a6**	**a7**	**a8**	**a9yel**	**a9or**	**a10**	**a11**
Formula	$C_{20}H_{13}Cl_3N_2OSn$	$C_{21}H_{15}Cl_3N_2OSn$	$C_{16}H_{10}Cl_3N_3O_3Sn$	$C_{16}H_{11}Cl_3N_2OSn$	$C_{16}H_9Cl_5N_2OSn$	$C_{16}H_{11}Cl_3N_2O_2Sn$	$C_{16}H_{10}Cl_3FN_2OSn$	$C_{16}H_{10}Cl_3FN_2OSn$	$C_{17}H_{13}Cl_3N_2O_2Sn$	$C_{20}H_{17}Cl_3N_2O_2Sn$
FW	522.38	536.41	517.32	472.32	541.21	488.32	490.32	490.32	502.35	542.42
Crystal system	triclinic	monoclinic	triclinic	monoclinic	triclinic	triclinic	monoclinic	monoclinic	monoclinic	monoclinic
Space group	$P\bar{1}$ (#2)	$P2_1/c$ (#14)	$P\bar{1}$ (#2)	$P2_1/c$ (#14)	$P\bar{1}$ (#2)	$P\bar{1}$ (#2)	$P2_1/n$ (#14)	$P2_1/c$ (#14)	$P2_1/c$ (#14)	$P2_1/c$ (#14)
a/Å	7.863(2)	13.028(5)	7.176(2)	12.768(5)	7.252(2)	7.379(5)	8.0700(5)	12.481(9)	7.181(1)	7.519(3)
b/Å	8.673(2)	11.405(3)	8.859(3)	7.069(3)	8.896(3)	10.410(6)	10.8801(7)	7.100(5)	16.472(3)	16.573(7)
c/Å	14.075(4)	15.174(5)	14.621(5)	17.981(7)	14.742(4)	11.333(7)	19.3363(11)	18.344(13)	15.316(2)	15.918(7)
α/degree	102.444(10)	90.000	99.798(3)	90.000	75.814(8)	79.665(19)	90.000	90.000		
β/degree	96.098(13)	113.296(6)	99.691(4)	102.446(5)	76.280(7)	75.118(16)	101.234(2)	103.068(5)	102.58(2)	100.477(6)
γ/degree	100.896(8)	90.000	99.296(3)	90.000	82.886(9)	74.92(2)	90.000	90.000		
V/Å^3	909.5(4)	2070.8(12)	885.3(5)	1584.7(10)	893.6(5)	806.4(9)	1665.24(18)	1583.3(19)	1768.1(4)	1950.4(15)
Z	2	4	2	4	2	2	4	4	4	4
D_{calcd}/g cm^{-3}	1.907	1.720	1.940	1.980	2.011	2.011	1.956	2.057	1.834	1.847
μ (Mo Kα)/cm^{-1}	18.582	16.347	19.171	21.209	21.834	20.919	20.305	21.356	19.083	17.401
Reflns collected	8807	22162	10090	15456	7692	8219	18463	17000	16796	22418
Unique reflns	4032	5752	4966	3887	3732	3856	4725	4548	4006	5598
R_{int}	0.043	0.042	0.021	0.029	0.025	0.025	0.048	0.057	0.031	0.033
G.O.F.	1.013	0.995	1.006	1.007	1.011	1.011	1.010	1.004	1.001	1.006
R_1 ($I > 2.00\sigma(I)$)[a)]	0.0354	0.0257	0.0223	0.0229	0.0322	0.0265	0.0245	0.0299	0.0292	0.0354
R; wR_2[b)]	0.0474; 0.0943	0.0296; 0.0642	0.0239; 0.0557	0.0251; 0.0538	0.0340; 0.0780	0.0291; 0.0634	0.0251; 0.0634	0.0302; 0.0781	0.0304; 0.1275	0.0403; 0.0752

a) $R_1 = \Sigma||F_o| - |F_c||/\Sigma|F_o|$. b) $wR_2 = [\Sigma(w(F_o^2 - F_c^2)^2)/\Sigma w(F_o^2)^2]^{1/2}$.

Regarding **a8**, strong intermolecular hydrogen bonds cause dimerization of the molecules as shown in Figure 2. As is expected in **a10**, the hydrogen bonds disappeared by the introduction of an OCH_3 group in place of the OH group in **a8**. No such strong hydrogen bonds are present in any other complex. Regarding **a9yel**, weak C–H···F and C–H···Cl interactions are present, while in **a9or**, π–π stackings exist between neighbor molecules (Figure 3). The dihedral angle of **a3** is larger than that of **a1** but has the same framework, which is probably due to the steric hindrance between the methyl group and chloride ion. The angles of **a8** and **a9yel** are also large compared to others, probably due to hydrogen bonds with the neighboring molecules. Incidentally, a complex $[SnCl_3(H_2O)(L6)]$[13] having similar composition to that of **a6** was reported (Chart S2). The former was synthesized in ethanol, and its structure was determined by infrared spectroscopy.

Electronic Spectra, Fluorescence Spectra, and Fluorescence Lifetimes of Schiff Base Ligands and Schiff Base Tin(IV) Complexes. Photophysical data of Schiff bases and Schiff base tin complexes in DMSO at room temperature are summarized in Table 4. The data of the unisolated ligands **HL6**, **HL9**, and **HL11** are not included in the table. The ligand **HL5** is unstable in DMSO, and only the datum of the solid-state emission is included. Electronic spectra of Schiff base ligands are shown in Figure S2. The table and the spectra show that the ligands **HL1**–**HL7** have absorption peaks in the visible region while **HL8** does not; they also show that the spectra of **HL1**–**HL3**, which have naphthalene moieties, have large absorption peaks in the 450–550 nm region. ^{1}H NMR spectra indicate that **HL1**–**HL7** are in the keto form in DMSO, while **HL8** is in the enol form. It has been reported that the keto forms have absorption bands in the visible region, while the enol forms do not.[27] Schiff base ligands are not fluorescent in DMSO, except **HL4′**, and are fluorescent in solids. The complexes **a1**–**a7** are fluorescent both in solutions and solids. Probably coordination of the ligands decreases their flexibility, which reduces the vibrations of the ligands. The planarities and fluorescence magnitudes of Schiff bases of the complexes have no correlation.

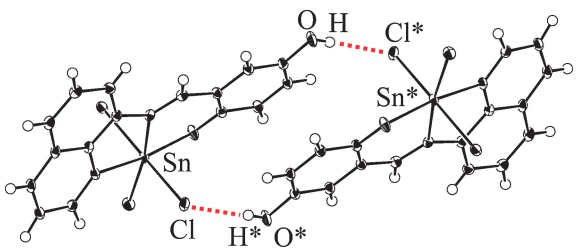

Figure 2. Partial packing diagram of **a8** showing hydrogen bonds. O–H, 0.91 Å; H–Cl*; 2.27 Å, O–H···Cl*: 175.4°; symmetry operator: (*) $-X+1$, $-Y+1$, $-Z+1$.

Electronic spectra of **a1**–**a11** are shown in Figures 4a and 4b. Most of the Schiff base complexes have their characteristic peaks at around 360 and 450 nm. The lowest excited singlet (S_1) and second excited singlet (S_2) states for these ligands are $^1\pi\pi^*$ in character because the molar extinction coefficients for these ligands are large, 5000–27000 M^{-1} cm^{-1} at the absorption peak wavelengths and tin(IV) complexes such as $SnCl_4$ and $[SnCl_6]^{2-}$ do not show any absorption in near ultraviolet and visible regions. In DMSO, the molar extinction coefficients for these tin complexes are also large, 4800–18000 M^{-1} cm^{-1} at the absorption peak wavelengths. Therefore, the S_1 and S_2 states for these complexes will also be $^1\pi\pi^*$ in character.

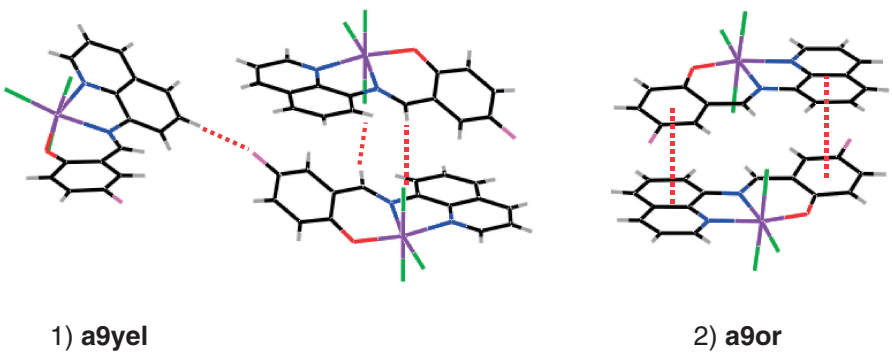

Figure 3. Partial packing diagrams of **a9yel** and **a9or**.

Table 3. Selected Bonds Length (Å) and Dihedral Angles (°) for **a1**, **a3**, **a5**, **a6**, **a7**, **a8**, **a9yel**, **a9or**, **a10**, and **a11**

	Sn1–Cl1	Sn1–Cl2	Sn1–Cl3	Sn1–N11	Sn1–N21	Sn1–O21	Dihedral ang.
a1	2.437(1)	2.408(1)	2.368(1)	2.186(3)	2.180(3)	2.024(3)	2.8
a3	2.4605(7)	2.4458(7)	2.4027(7)	2.290(2)	2.193(2)	2.069(2)	25.9
a5	2.4139(8)	2.4001(8)	2.3639(8)	2.187(2)	2.179(2)	2.034(1)	6.0
a6	2.4075(8)	2.4142(8)	2.3634(8)	2.201(2)	2.181(2)	2.019(2)	8.8
a7	2.407(1)	2.420(1)	2.367(1)	2.182(3)	2.185(3)	2.020(2)	0.5
a8	2.425(1)	2.441(1)	2.348(1)	2.187(2)	2.192(2)	2.003(2)	15.6
a9yel	2.4210(5)	2.3945(5)	2.3530(5)	2.200(2)	2.189(2)	2.020(1)	28.3
a9or	2.384(1)	2.421(1)	2.357(1)	2.195(2)	2.191(2)	2.014(2)	10.7
a10	2.396(3)	2.438(3)	2.350(3)	2.212(4)	2.149(3)	2.029(4)	1.9
a11	2.407(1)	2.405(1)	2.366(1)	2.202(2)	2.170(2)	2.016(2)	4.0

Table 4. Photophysical Data of Schiff Bases **HL1**–**HL3**, **HL4′**, **HL5**, **HL7**–**HL10** and Schiff Base Tin Complexes **a1**–**a11** in DMSO and in Solid State at Room Temperature

Compd	Absorbance λ_{max}/nm (ε/M^{-1} cm^{-1})	Emission soln (QY)[a),b)]	Stokes shift /cm^{-1}	Emission in solid state[c)]
HL1	457 (23100), 481 (24400)	no emission	—	553
HL2	470 (24800), 496 (23100)	no emission	—	589
HL3	457 (25600), 481 (27000)	no emission	—	557
HL4′	350 (26400), 504 (7700)	483	—	594
HL5	—[d)]	—[d)]	—	570
HL7	531 (5290)	no emission	—	586
HL8	400sh (6620)	no emission	—	no emission
HL10	355 (8100)	—		
a1	366 (9340), 453 (17700)	515 (0.21)	2660	555
a2	360 (16600), 470 (16200)	545 (0.025)	2930	586
a3	363 (9620), 450 (18000)	509 (0.13)	2580	546
a4	347 (15300), 435 (11700)	538 (0.042)	4400	563
a5	402 (14900)	492 (0.022)	4550	523
a6	343 (15200), 421 (12900)	518 (0.028)	4450	536
a7	348 (14700), 429 (9700)	540 (0.046)	4790	553
a8	355 (17000), 476 (8170)	no emission	—	no emission
a9yel	360sh (8090), 430 (9050)	535 (0.058)	4560	540
a9or	360sh (8090), 430 (9050)	535 (0.058)	4560	549
a10	351 (13400), 464 (8430)	no emission	—	584
a11	368 (17500), 450 (4810)	no emission	—	590

a) Emission λ_{max}/nm (quantum yield, QY) in a DMSO solution: 1.0×10^{-5} mol L^{-1}, $\lambda_{ex} = 390$ nm. b) Standard: a DMF solution of Alq_3,[25b] $\lambda_{ex} = 390$ nm. c) Emission λ_{max}/nm. d) Unstable in DMSO.

Normalized fluorescent spectra of **a1**–**a7** are shown in Figure 5. Table 4 also contains fluorescent data of the ligands and complexes in solutions and in solid states. Solid samples show fluorescence at longer wavelengths than solution samples (Figure S3). The electronic, fluorescence, and ^{1}H NMR spectra of **a9yel** and **a9or** in DMSO agree fully with each other. The complexes **a8**, **a10**, and **a11** do not show fluorescence in DMSO. Especially **a8** does not show fluorescence even in the solid state, while **a10** and **a11** show fluorescence in the solid states. The dimerization of **a8** by hydrogen bonds is most probably the cause of its nonfluorescence in solid, and the interaction of **a8**, **a10**, and **a11** with DMSO is likely the cause of their nonfluorescence. The dimerized form of **a8** may also be present in DMSO.

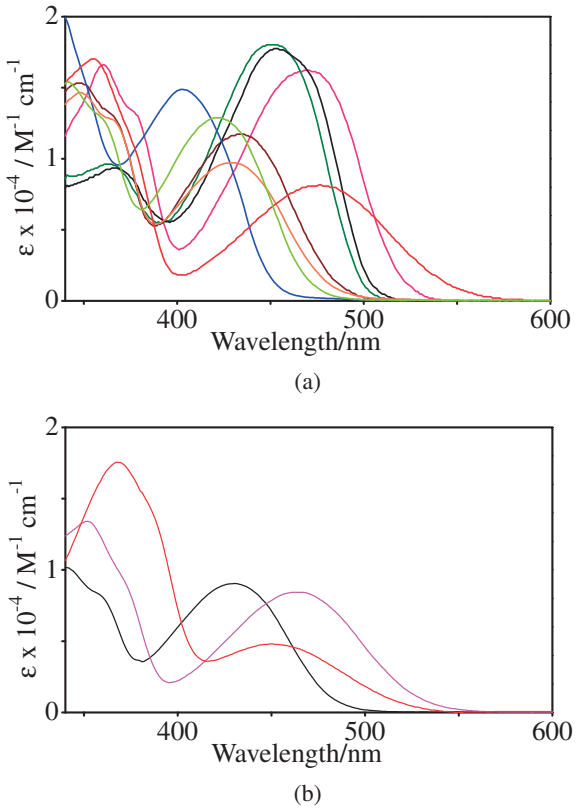

Figure 4. (a) Electronic spectra of **a1** (—), **a2** (—), **a3** (—), **a4** (—), **a5** (—), **a6** (—), **a7** (—), and **a8** (—) in DMSO. (b) Electronic spectra of **a9** (—), **a10** (—), and **a11** (—) in DMSO.

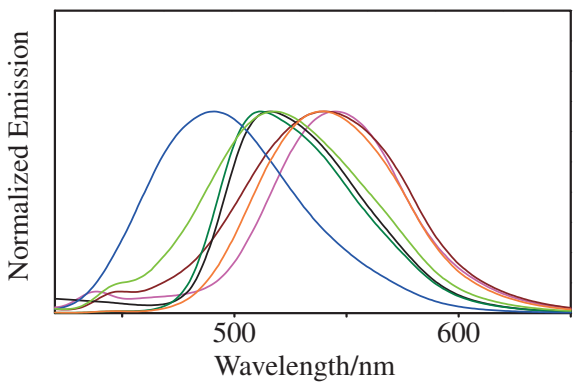

Figure 5. Emission spectra of **a1** (—), **a2** (—), **a3** (—), **a4** (—), **a5** (—), **a6** (—), and **a7** (—) in DMSO at room temperature ($\lambda_{ex} = 390$ nm).

The alteration of ligands led to fairly large changes of fluorescence peak wavelength. This demonstrates that the emission wavelength of tin(IV) complexes is tunable by ligand modification.[1c,28] The emission wavelengths (λ_{max}) of the fluorenecarboxylato tin complexes are 355 and 390 nm,[14] while that of the tin–iridium complex is 645 nm;[15] the emission wavelengths (492–545 nm) of the present Schiff base tin complexes are between those of the two types of complexes.

The fluorescence quantum yields (Φ_f) of each complex were determined by eq 1.[29]

Table 5. Fluorescence Lifetimes of Tin Complexes in DMSO at Room Temperature

Compd	τ/ns	χ^2	k_f/ns^{-1}	k_{nr}/ns^{-1}
a1	1.76	1.616	0.119	0.449
a2	0.49	1.120	0.0510	1.989
a3	1.36	1.428	0.0955	0.639
a4	0.86	1.339	0.0488	1.114
a6	0.78	1.306	0.0359	1.246
a7	1.10	1.412	0.0418	0.867

$$\frac{\Phi_f}{\Phi_r} = \frac{F_f}{F_r}\frac{A_r}{A_f}\frac{{n_f}^2}{{n_r}^2} \quad (1)$$

where F is the integrated fluorescence intensity, Φ is the quantum yield, A is the absorbance, n is the refractive index for solvent, and the subscripts f and r represent the complex sample solutions and the reference solution, respectively. The Φ_r value for reference complex, **Alq$_3$**, in DMF is 0.11.[25b] After the photoirradiation, the complexes are excited to the first excited state. The first excited state decays to the ground state by the radiative (fluorescent) and/or nonradiative (thermal) relaxation processes. The fluorescence lifetimes of complexes **a1**–**a7** were measured. Complex **a5** was not stable enough to get the lifetime. The time-resolved fluorescence intensities are described as the single exponential function (eq 2):

$$F = F_0 \exp(-t/\tau) \quad (2)$$

where τ is the lifetime of the excited state. The fluorescent and nonradiative rate constants are described as

$$k_f = \Phi_f/\tau \quad (3)$$

$$k_{nr} = \Phi_{nr}/\tau \quad (4)$$

$$\Phi_f + \Phi_{nr} = 1 \quad (5)$$

where k is the rate, Φ is the quantum yield, and the subscripts f and nr represent the fluorescent and nonradiative relaxation processes, respectively (eqs 3–5).

The fluorescence lifetimes (ca. 1.8–0.5 ns) of **a1**–**a4**, **a6**, and **a7** are relatively small and summarized in Table 5. Plots of lifetime/ns vs. quantum yield, k_f vs. quantum yield, and k_{nr} vs. quantum yield are shown in Figures S4a, S4b, and S4c, respectively. The table and figures indicate the following: 1) Complexes **a1** and **a3** have relatively large quantum yields, and their fluorescence rate constants k_f's are similar to each other, while k_{nr} of **a1** is less than that of **a3**. The introduction of a methyl group to the ligand **HL1** gives **HL3**, and the stretching vibration of the quinoline ring-methyl group will cause deactivation of **a3**. 2) Complexes **a4**, **a6**, and **a7** have relatively small quantum yields, and their k_f's and k_{nr}'s are similar to each other. 3) Complex **a2** has small quantum yields, and the magnitude of k_f is similar to that of other complexes, but the magnitude of k_{nr} is larger than that of any other complexes. Probably, the orientation change of the naphthalene ring from **HL1** to **HL2** causes loss of activated energy through vibration. 4) The Stokes shifts of **a1**, **a2**, and **a3** which have naphthalene rings are ca. 2700 cm^{-1}, while those of **a4**, **a6**, **a7**, and **a9** which have benzene rings are ca. 4500 cm^{-1}. It is clear that the fluorescence quantum yields and Stokes shifts have no correlation ship.

Table 6. HOMO–LUMO Gaps Obtained by DFT Calculations (B3LYP/6-31G**; Sn, LanL2DZ)

Compd	HOMO /eV	LUMO /eV	HOMO–LUMO gap/eV
a1	−6.05	−3.01	3.04
a2	−5.81	−3.01	2.80
a3	−6.01	−2.86	3.15
a4	−6.03	−3.01	3.02
a5	−6.80	−3.47	3.34
a6	−6.23	−3.09	3.14
a7	−6.35	−3.35	3.00
a8	−5.82	−3.21	2.61
a9	−6.20	−3.20	3.00
a10	−5.71	−3.05	2.66
a11	−5.66	−2.97	2.69

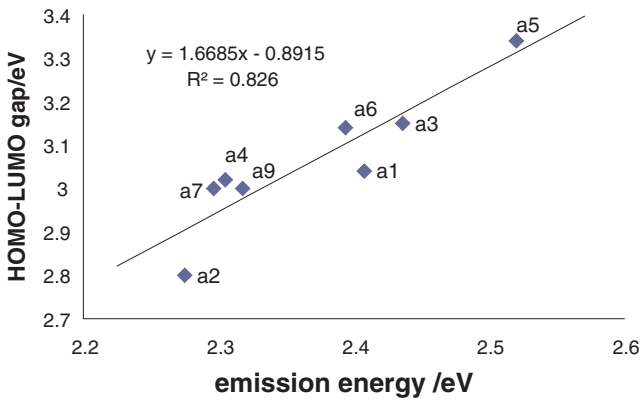

Figure 6. Plots of emission wavelengths vs. HOMO–LUMO gaps for **a1**–**a7** and **a9**.

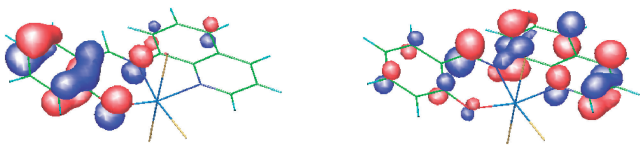

Figure 7. Visualized frontier orbitals for **a6**.

DFT Calculation. DFT calculations show that the order of the magnitudes of HOMO–LUMO gaps (Table 6) is consonant with that of the emission wavelengths (λ_{max}) of the complexes as shown in Figure 6. It is common knowledge that the fluorescence wavelength depends on both excited and ground states, however, the wavelength is predictable in the case of these Schiff base complexes.

Frontier orbitals of all the complexes show that the main components of HOMO's are aldehyde moieties and those of LUMO's are quinoline moieties. The frontier orbitals of **a1** (Figure S5) and **a6** (Figure 7) are shown, for example, together with energy diagram of **a6** (Figure S6). The molecular orbital coefficients of **a6** indicate that the main atomic components of HOMO are C23 and C25, and those of LUMO are C11, C13, and C16: the atom numbering scheme of **a6** employed here is the same as that shown in Figure 1. Therefore the introduction of either electron-donating or -withdrawing groups into some

Table 7. Comparison of Cathodic Peak Potentials E^1_{pc} for Reduction of Schiff Bases and Schiff Base–Tin(IV) Complexes, and Sums of *para*- and *ortho*-Substituted Hammett Parameters

Compd	E^1_{pc}/V vs. Fc/Fc^+	*p*-	σ_p	*o*-	σ_o	$\sigma_p + \sigma_o$
HL1	−1.87	—	—	—	—	—
HL2	−1.88	—	—	—	—	—
HL3	−1.88	—	—	—	—	—
HL4′	−1.50	—	—	—	—	—
HL7	−1.56	—	—	—	—	—
HL8	−1.98	—	—	—	—	—
a1	−1.32	—	—	—	—	—
a2	−1.32	—	—	—	—	—
a3	−1.36	—	—	—	—	—
a4	−1.32	CH_3	−0.17	$CH(OCH_3)_2$	—	—
a5	−1.17	NO_2	+0.78	H	0.00	+0.78
a6	−1.32	H	0.00	H	0.00	0.00
a7	−1.15	Cl	+0.23	Cl	+0.37	+0.60
a8	−1.35	OH	−0.37	H	0.00	−0.37
a11	−1.34	$CH_2CH{=}CH_2$	−0.14	OCH_3	−0.24	−0.38

of the atoms (C11, C13, C16, C23, and C25) will cause the wavelength change of **a6**. The introduction of a nitro group (**a5**) or chlorine atoms (**a7**) to **a6** lowers both the energies of HOMO and LUMO. The nitro group and chlorine atoms have similar effects of lowering the HOMO of **a6**, but the nitro group has larger effect of lowering the HOMO of **a6** than the chlorine atoms have. As a result, larger HOMO–LUMO gap appears in the case of **a5**.

Electrochemistry. Cyclic voltammetry (CV) was used to determine the reduction potentials for the ligands and the complexes. For the purpose of an influence of ligand modifications on the electrochemical properties, these measurements were undertaken using a uniformed dimethyl sulfoxide (DMSO) solution containing 0.1 M tetrabutylammonium hexafluorophosphate (Bu_4NPF_6) with a scan rate of $0.1\,V\,s^{-1}$. All cyclic voltammograms exhibited irreversible waves and these results suggest that the reduction products of the ligands and the complexes were unstable under a time scale in CV measurements (Figures S7a, S7b, and S7c).

The cathodic peak potentials (E^1_{pc}) for reduction of the Schiff bases **HL1**–**HL3**, **HL4′**, **HL7**, and **HL8** and Schiff base tin(IV) complexes, and relevant Hammett parameters are listed in Table 7. The **HL5** ligand decomposed in DMSO and the **HL6** ligand was not isolated as a solid, and CV measurements of them were not conducted. The chemical structures of **HL1** and **HL2** have an isomeric relation. Therefore, the reduction potentials of these two ligands were quite similar. The chemical structure of **HL3** and **HL1** differs with regard to the methyl group. The substituent has little influence on the reduction potential. The reduction potentials of Schiff base tin(IV) complexes were more positive than these corresponding free Schiff base ligands. DFT calculations for these complexes indicate that all LUMO are distributed to the ligands and the reductions are considered to occur at the ligand moiety. These results suggest that these enolates, which are generated by the complexations, have more easily reduced moieties and the differences among these five complexes are due to the influence of the substituent groups.

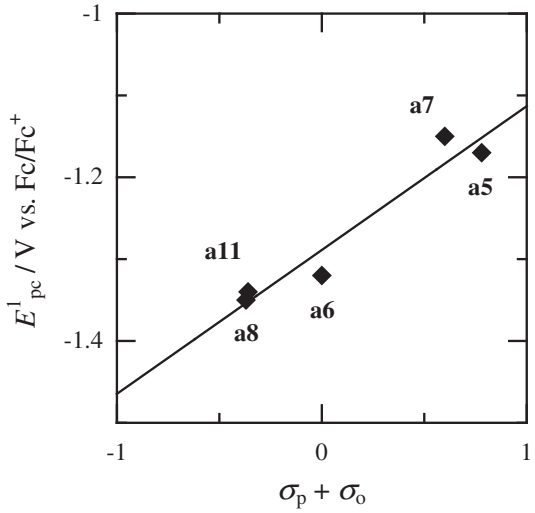

Figure 8. Correlation between first reduction peak potentials (E^1_{pc}) and sums of *para*- (σ_p) and *ortho*-substituted (σ_o) Hammett parameters.

Correlation between Hammett Parameters and Electrochemistry. As for the complexes **a5**, **a6**, **a7**, **a8**, and **a11** in Table 7, the substituents are considered to be in a *para*- and *ortho*-position with respect to the phenolic oxygen, and the *para* σ_p[30]- and *ortho* σ_o[31]-substituted Hammett parameters are as noted in Table 7. There is a good linear relationship between the sum of the σ_p and σ_o values and the E^1_{pc} values ($R^2 = 0.93$, Figure 8) and the larger sum of the σ_p and σ_o values corresponds the larger E_{pc} value. Generally, substituents with a plus σ value are electron-withdrawing groups and the larger σ value renders the reduction easier.[32–34] These electrochemical results confirm that substituents, which are in the *para*- and *ortho*-positions with respect to the phenolic oxygen of the Schiff base ligands, affect the electronic structures of the complexes.

Correlation between Theoretical Studies and Electrochemistry. In the case of the one-electron-reduction process,

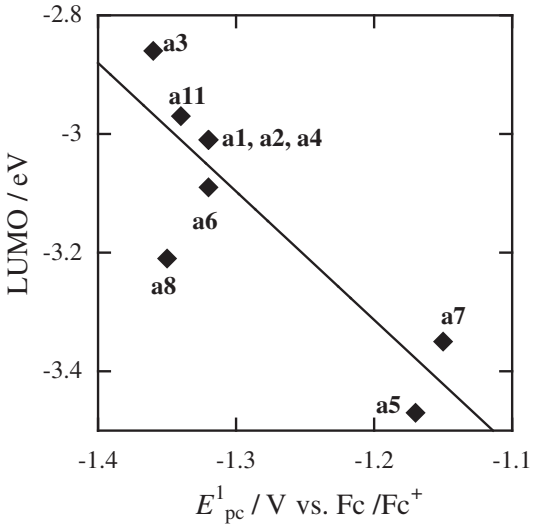

Figure 9. Correlation between LUMO energies and first reduction peak potentials (E^1_{pc}).

an electron flows from an electrode to a LUMO and the standard potential, E^0, is known to be related to a LUMO energy level.[35] Plots of first cathodic peak potentials of a series of the complexes versus LUMO energy level, which are the results of density functional theory (DFT) calculations, showed a correlation ($R^2 = 0.73$, Figure 9). The crystal structure of **a8** shows that strong hydrogen bonds between two adjacent **a8** molecules form a pseudo dinuclear complex (see the crystal structure of **a8**). This can be one of the reasons for the deviation of **a8** from the correlation.

Summary

Eleven Schiff base tin(IV) complexes **a1**–**a11** of the types [$SnCl_3$(L)] (HL: Schiff base) were synthesized and characterized especially for fluorescence. All except **a8**, **a10**, and **a11** are fluorescent in DMSO (λ_{max}/nm: 492–545 nm). The fluorescence quantum yields (Φ_f) of the complexes depend very much on the ligands ($\Phi_f = 0.21$–0.022). Of the solids, **a10** and **a11** are fluorescent, but **a8**, the ligand having an OH group, is not. The fluorescence lifetimes ($\tau = 0.49$–1.76 ns) of **a1**–**a4**, **a6**, and **a7** are relatively small. The DFT calculation shows that the order of the magnitudes of HOMO–LUMO gaps is consonant with that of the emission wavelengths (λ_{max}) of the complexes, and the emission wavelength is predictable in the case of these Schiff base tin complexes. The cyclic voltammograms indicate that reduction products of the complexes are unstable under the time scale in CV measurements (0.1 V s^{-1}). A relatively good correlation except for **a8** was observed between reduction potentials in DMSO and the energies of LUMO.

We thank Profs. S. Toyota and H. Yamada of Okayama University of Science for helpful discussions of the NMR spectra.

Supporting Information

Additional spectroscopic, electrochemical, and DFT data and line drawings of related compounds. This materital is available free of charge on the Web at: http://www.csj.jp/journals/bcsj/.

References

1 a) *Organic Electroluminescence*, ed. by Z. H. Kafafi, CRC Press, **2005**. b) C. H. Chen, J. Shi, *Coord. Chem. Rev.* **1998**, *171*, 161. c) S. Minakata, S. Moriwaki, H. Inada, M. Komatsu, H. Kajii, Y. Ohmori, M. Tsumura, K. Namura, *Chem. Lett.* **2007**, *36*, 1014. d) J. Yoshino, N. Kano, T. Kawashima, *Chem. Commun.* **2007**, 559.

2 For example: a) R. Danaboyina, J. Kuthanapillil, T. A. Kalliat, PCT Int. Appl. 24, **2007**. b) R. Paul, A. Kiuro, K.-O. Söderström, J. Tuominen, R. Johansson, M. Haaparanta, D. Roeda, O. Solin, *Life Sci.* **1987**, *40*, 1609.

3 C. Jiang, F. He, *Spectrochim. Acta, Part A* **2003**, *59*, 1321.

4 C. Jiang, H. Wang, J. Wang, *Anal. Lett.* **2001**, *34*, 1341.

5 C. Jiang, J. Wang, F. He, *Anal. Chim. Acta* **2001**, *439*, 307.

6 H. Wang, F. He, C. Jiang, *Analyst* **2001**, *126*, 1164.

7 J. Li, F. He, C.-q. Jiang, *Anal. Sci.* **2006**, *22*, 607.

8 G. Sakane, H. Kawasaki, T. Shibahara, *Acta Crystallogr., Sect. E: Struct. Rep. Online* **2006**, *62*, o2736.

9 G. Asgedom, A. Sreedhara, J. Kivikoski, E. Kolehmainen, C. P. Rao, *J. Chem. Soc., Dalton Trans.* **1996**, 93.

10 F. Tisato, F. Refosco, A. Moresco, G. Bandoli, U. Mazzi, M. Nicolini, *J. Chem. Soc., Dalton Trans.* **1990**, 2225.

11 D. Urakami, K. Inoue, S. Hayami, *Acta Crystallogr., Sect. E: Struct. Rep. Online* **2009**, *65*, m800.

12 a) Z. Luo, L. Liang, Z. Huang, Y. Cui, *Fenxi Huaxue* **2000**, *28*, 702. b) B. K. Pal, M. Ukiluddin, *J. Bangladesh Acad. Sci.* **1992**, *16*, 135. c) Y. Yamamoto, Y. Dohdan, K. Morishige, Y. Nishikawa, *Nippon Kagaku Kaishi* **1990**, *1*, 25. d) S. Rubio, A. Gómez-Hens, M. Valcárcel, *Analyst (Cambridge, U.K.)* **1985**, *110*, 43. e) M. Deguchi, K. Yokoyama, M. Umeda, Y. Sahei, K. Morishige, K. Yamaguchi, *Hiroshima Daigaku Kogakubu Kenkyu Hokoku* **1993**, *41*, 139. f) K. Morishige, *Kinki Daigaku Rikogakubu Kenkyu Hokoku* **1981**, 271. g) Among them, 2-hydroxy-5-sulfoaniline-*N*-salicylidene and *N*-salicylidene-2-hydroxy-5-carboxyaniline are Schiff bases.

13 A. M. Donia, H. El-Boraey, *Thermochim. Acta* **1994**, *237*, 195.

14 V. Chandrasekhar, P. Thilagar, A. Steiner, J. F. Bickley, *Chem.—Eur. J.* **2006**, *12*, 8847.

15 a) A. L. Balch, M. M. Olmstead, D. E. Oram, P. E. Reedy, Jr., S. H. Reimer, *J. Am. Chem. Soc.* **1989**, *111*, 4021. b) A. L. Balch, B. J. Davis, M. M. Olmstead, *Inorg. Chem.* **1990**, *29*, 3066.

16 a) T. Seifert, W. Storch, M. Vosteen, *Eur. J. Inorg. Chem.* **1998**, 1343. b) A. Hazell, K. F. Thong, J. Ouyang, L. E. Khoo, *Acta Crystallogr., Sect. C* **1997**, *53*, 1226. c) A. Bengtson, N. K. Goh, A. Hazell, L. E. Khoo, J. Ouyang, K. R. Pedersen, *Acta Chem. Scand.* **1996**, *50*, 1020.

17 X. T. Tao, M. Shimomura, H. Suzuki, S. Miyata, H. Sasabe, *Appl. Phys. Lett.* **2000**, *76*, 3522.

18 K. Takano, T. Shibahara, *Chem. Lett.* **2008**, *37*, 70.

19 M. Takezaki, T. Tominaga, *J. Photochem. Photobiol., A* **2005**, *174*, 113.

20 P. T. Beurskens, G. Admiraal, G. Beurskens, W. P. Bosman, S. Garcia-Granda, R. O. Gould, J. M. M. Smits, C. Smykalla, *The DIRDIF Program System*, Technical Report of the Crystallography Laboratory, University of Nijmegen, The Netherlands, **1992**.

21 SIR2004: M. C. Burla, R. Caliandro, M. Camalli, B. Carrozzini, G. L. Cascarano, L. De Caro, C. Giacovazzo, G. Polidori, R. Spagna, *J. Appl. Crystallogr.* **2005**, *38*, 381.

22 G. M. Sheldrick, *SHELXS-97, Program for the Solution of Crystal Structures*, University of Göttingen, Germany, **1997**.

23 P. T. Beurskens, G. Admiraal, G. Beurskens, W. Bosman, P. R. de Gelder, R. Israel, J. M. M. Smits, *The DIRDIF-99 Program System*, Technical Report of the Crystallography Laboratory, University of Nijmegen, The Netherlands, **1999**.

24 *Crystal Structure Analysis Package*, Rigaku and Rigaku/MSC, TX, USA, **2000–2006**.

25 a) J. Wang, K. D. Oyler, S. Bernhard, *Inorg. Chem.* **2007**, *46*, 5700. b) F. E. Lytle, D. R. Storey, M. E. Juricich, *Spectrochim. Acta, Part A* **1973**, *29*, 1357.

26 Gaussian 03 program package: M. J. Frisch, G. W. Trucks, H. B. Schlegel, G. E. Scuseria, M. A. Robb, J. R. Cheeseman, J. A. Montgomery, Jr., T. Vreven, K. N. Kudin, J. C. Burant, J. M. Millam, S. S. Iyengar, J. Tomasi, V. Barone, B. Mennucci, M. Cossi, G. Scalmani, N. Rega, G. A. Petersson, H. Nakatsuji, M. Hada, M. Ehara, K. Toyota, R. Fukuda, J. Hasegawa, M. Ishida, T. Nakajima, Y. Honda, O. Kitao, H. Nakai, M. Klene, X. Li, J. E. Knox, H. P. Hratchian, J. B. Cross, V. Bakken, C. Adamo, J. Jaramillo, R. Gomperts, R. E. Stratmann, O. Yazyev, A. J. Austin, R. Cammi, C. Pomelli, J. W. Ochterski, P. Y. Ayala, K. Morokuma, G. A. Voth, P. Salvador, J. J. Dannenberg, V. G. Zakrzewski, S. Dapprich, A. D. Daniels, M. C. Strain, O. Farkas, D. K. Malick, A. D. Rabuck, K. Raghavachari, J. B. Foresman, J. V. Ortiz, Q. Cui, A. G. Baboul, S. Clifford, J. Cioslowski, B. B. Stefanov, G. Liu, A. Liashenko, P. Piskorz, I. Komaromi, R. L. Martin, D. J. Fox, T. Keith, M. A. Al-Laham, C. Y. Peng, A. Nanayakkara, M. Challacombe, P. M. W. Gill, B. Johnson, W. Chen, M. W. Wong, C. Gonzalez, J. A. Pople, *Gaussian 03 (Revision E.01)*, Gaussian, Inc., Wallingford CT, **2004**.

27 For example, ref. 5.

28 C. Pérez-Bolívar, V. A. Montes, P. Anzenbacher, Jr., *Inorg. Chem.* **2006**, *45*, 9610.

29 a) J. N. Demas, G. A. Crosby, *J. Phys. Chem.* **1971**, *75*, 991. b) J. R. Lakowicz, *Principles of Fluorescence Spectroscopy*, 2nd ed., Springer, New York, **2004**. c) N. J. Turro, *Modern Molecular Photochemistry*, University Science Books, California, **1991**. d) D. M. Roundhill, *Photochemistry and Photphysics of Metal Complexes*, Prenum Press, New York, **1994**.

30 C. Hansch, A. Leo, R. W. Taft, *Chem. Rev.* **1991**, *91*, 165.

31 R. W. Taft, Jr., *J. Am. Chem. Soc.* **1952**, *74*, 3120.

32 H.-J. Son, W.-S. Han, J.-Y. Chun, B.-K. Kang, S.-N. Kwon, J. Ko, S. J. Han, C. Lee, S. J. Kim, S. O. Kang, *Inorg. Chem.* **2008**, *47*, 5666.

33 D. Donghi, G. D'Alfonso, M. Mauro, M. Panigati, P. Mercandelli, A. Sironi, P. Mussini, L. D'Alfonso, *Inorg. Chem.* **2008**, *47*, 4243.

34 P. Zanello, *Inorganic Electrochemistry: Theory, Practice and Application*, The Royal Society of Chemistry, Cambridge, U.K., **2003**, pp. 579–589. doi:10.1039/9781847551146-00579.

35 A. J. Bard, L. R. Faulkner, in *Electrochemical Methods: Fundamentals and Applications*, 2nd ed., John Wiley & Sons, Inc., **2001**, pp. 4–5.